Available online at www.sciencedirect.com
SCIENCE DIRECT®
Thermochimica Acta 417 (2004) 59–65
thermochimica acta
www.elsevier.com/locate/tca

# Gibbs free energy of formation of calcium rhodite

Aparna Banerjee, R. Prasad*, V. Venugopal

*Fuel Chemistry Division, Bhabha Atomic Research Centre, Trombay, Mumbai 400085, India*

Received 14 August 2003; accepted 24 December 2003

Available online 5 March 2004

**Abstract**

The Gibbs free energy of formation of $CaRh_2O_4$(s) has been determined using two techniques viz., quadrupole mass spectrometer coupled to a Knudsen cell and solid-state cell incorporating $CaF_2$(s) as the solid electrolyte. In the former method, equilibrium $O_2$(g) pressures were measured over the phase field Rh(s) + $Rh_2O_3$(s), in the temperature range 793.7–909.1 K and over the three phase mixture $CaRh_2O_4$(s) + Rh(s) + CaO(s) was measured from 862.1 to 1022.7 K.

The Gibbs free energy of formation of $Rh_2O_3$(s) from elements in their standard state can be given by

$\Delta_f G^\circ(Rh_2O_3(s))\ (kJ\,mol^{-1} \pm 2.0) = -363.2 + 0.241T\ (K).$

The Gibbs free energy of formation of $CaRh_2O_4$(s) from elements in their standard state can be given by

$\Delta_f G^\circ(CaRh_2O_4(s))\ (kJ\,mol^{-1} \pm 2.0) = -1030.5 + 0.3437T\ (K).$

In the electrochemical technique, the cell configuration employed was

$(-)Pt/O_2(g), \{CaO(s) + CaF_2(s)\}//CaF_2//\{CaRh_2O_4(s) + Rh_2O_3(s) + CaF_2(s)\}, O_2(g)/Pt(+).$

The emf values were measured in the temperature range 879.7–1000 K can be represented by the following expression:

$E\ (V)(\pm 7.63 \times 10^{-4}) = 0.3928 - 2.374 \times 10^{-4}T\ (K).$

From the measured emf of the cell and requisite $\Delta_f G^\circ$ values from the literature, $\Delta_f G^\circ(CaRh_2O_4(s))$ from elements in their standard state has been calculated and can be represented by $\Delta_f G^\circ(CaRh_2O_4(s))\ (kJ\,mol^{-1} \pm 2.0) = -1079 + 0.390T\ (K)$.

The uncertainty estimates for $\Delta_f G^\circ$ include the standard deviation in the emf and uncertainty in the data taken from the literature. The slope and intercept of the above equation gives the entropy and enthalpy of formation of the compound at the average experimental temperature $T_{av} = 940$ K.


*Keywords:* System Ca–Rh–O; Gibbs energy of formation; Quadrupole mass spectrometric technique; Solid-state electrochemical technique

## 1. Introduction

Thermodynamics of inter-oxide compounds are important for defining the nature of interaction of platinum group metals with refractory oxides and the conditions under which these metals can be lost in high temperature processes [1]. The role of rhodium in catalytic reactions is closely related to the formation of rhodium oxides. Knowledge of the formation of rhodium oxides and other platinum group metal oxides is important for understanding the nature of catalytic processes [2]. Understanding the thermodynamic properties of rhodites is important to determine their behavior during operation, accident and in high-temperature waste immobilisation process [3]. Skrobot [4] identified an inter-oxide compound $CaRh_2O_4$(s) in the pseudo-binary system CaO–$Rh_2O_3$. The physico-chemical properties of $Rh_2O_3$(s) and $CaRh_2O_4$(s) were determined in order to design processes to recover the precious metal from scrap. Several workers [5–8] have determined the

* Corresponding author. Fax: +91-22-25505151.
*E-mail address:* prasadr@apsara.barc.ernet.in (R. Prasad).

0040-6031/$ – see front matter © 2004 Elsevier B.V. All rights reserved.
doi:10.1016/j.tca.2003.12.028

$\Delta_f G^\circ$ of $Rh_2O_3$(s) by using galvanic cell. However, there is considerable disagreement in their data and hence it was decided to redetermine $\Delta_f G^\circ$ of $Rh_2O_3$(s) by an independent technique viz. quadrupole mass spectrometer (QMS) coupled to a Knudsen cell in the temperature range from 793.7 to 909.1 K. There is only one report in the literature [9] for the determination of $\Delta_f G^\circ$ of calcium rhodite by solid state electrochemical cell. $\Delta_f G^\circ$ of calcium rhodite was determined in the temperature range 862.1–1022.7 K by QMS coupled to a Knudsen cell. The thermodynamic properties of calcium rhodite was also determined and further refined by determining the Gibbs free energy by solid state galvanic cell using $CaF_2$(s) as the solid electrolyte in the temperature range 879.7–1000 K.

## 2. Experimental

### 2.1. Materials

Rhodium metal was prepared by passing $Ar/H_2$ gas over $RhCl_3$(s) (Johnson Matthey, England) at 1023 K. $Rh_2O_3$(s) was prepared from $RhCl_3$(s) by passing oxygen gas at 1023 K. This gave ($\alpha$) $Rh_2O_3$(s) which on heating at 1273 K gave the ($\beta$) phase. For the preparation of $CaRh_2O_4$(s) the only compound in the Ca–Rh–O system, stoichiometric proportions of $CaCO_3$(s) (99.7 mass%, BDH, Poole, UK) and $Rh_2O_3$(s) were mixed, pulverised thoroughly and calcined at 1173 K for 1 week. This mixture was pulverised again, pelletised and heated to1473 K for several days with intermediate grindings. $CaRh_2O_4$(s) was characterised as a pure phase by X-ray diffraction technique. The values of the interplanar spacing $d$ obtained in the present study using a DIANO X-ray diffractometer is in good agreement with those reported in JCPDS-file # 41-542. Phase mixtures {$Rh_2O_3$(s) + Rh(s)} and {$CaRh_2O_4$(s) + Rh(s) + CaO(s)} were pelletised and sintered in argon at 1000 K for a week and used for measurements.

### 2.2. Knudsen effusion cell–quadrupole mass spectrometer assembly

The experimental assembly comprising of a QMS coupled to the Knudsen effusion cell has been represented schematically in Fig. 1. The QMS has a resolution of 1 amu. The detector part consists of a particle multiplier of conversion dynode type. The Knudsen effusion cell assembly was coupled to the quadrupole mass analyser system through a CF-100 port by Cajon coupling. The cell assembly is arranged in such a manner that the effusing beam from the Knudsen cell strikes the ioniser at right angles. The Knudsen effusion cell used had a height of 0.015 m, 0.011 m diameter with an orifice placed in the center of the lid. The orifice diameter was $7.0 \times 10^{-4}$ m, and the area of the orifice was determined by measuring the average diameter of the orifice using an optical microscope. The cell and the lid were made of 15 mol% calcia-stabilised-zirconia. The Knudsen effusion cell was kept inside a quartz container which was heated to the desired temperature using a Kanthal wire wound furnace. A turbo molecular pump backed up by a direct driven rotary pump yielded a vacuum better than $10^{-5}$ Pa. The sample in the cell was then heated to 500 K to remove any

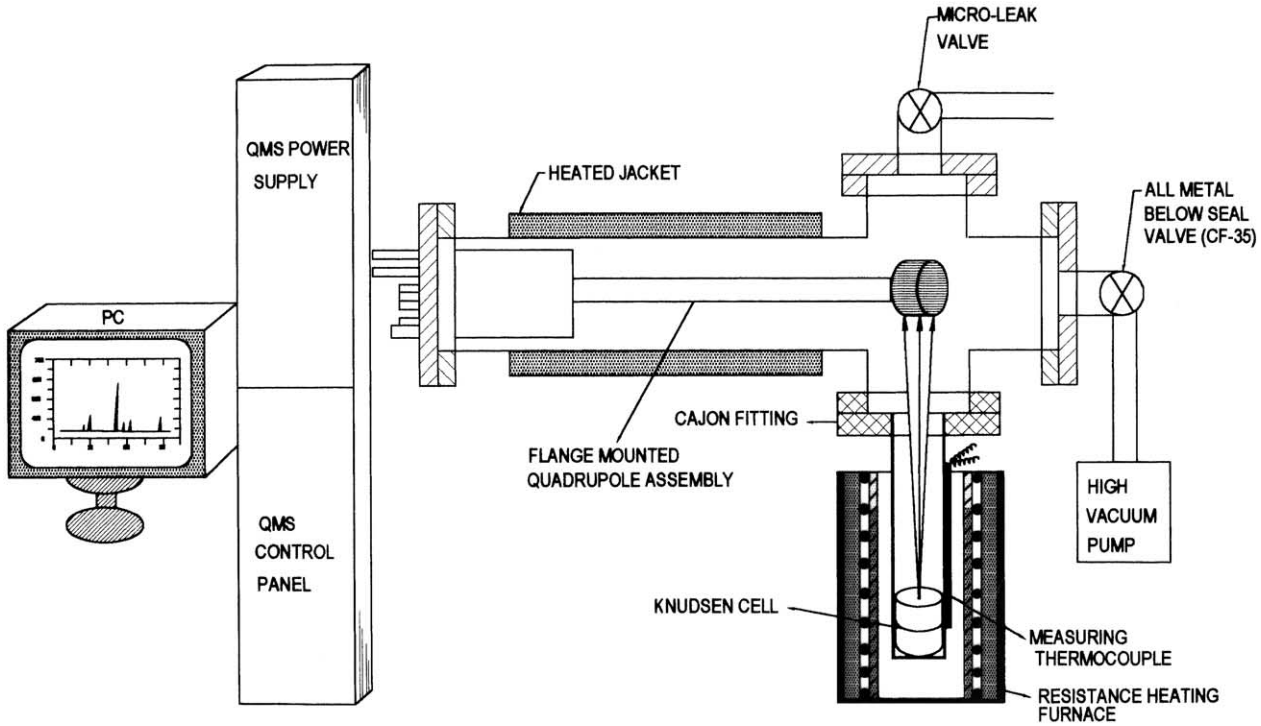


Fig. 1. Schematic diagram of the Knudsen effusion cell coupled to the quadrupole mass spectrometer.

trapped gases and moisture and then the temperature was raised to the desired value. The temperature of the furnace was monitored by a calibrated chromel-to-alumel thermocouple (±1 K). In this method, the vapor in equilibrium with one or more condensed phase is sampled without disturbing the equilibrium conditions and ionised in an electron impact ion source, mass analysed by quadrupole.

The partial pressure of the species is related to the measured ion intensity $I_i^+$ by the relation

$$P_i = \frac{KI_i^+ T}{\sigma_i} \quad (1)$$

where the subscript $i$ refers to the $i$th species, $K$ is the instrument constant $I$ is the measured ion current, $T$ is the absolute temperature of the Knudsen source and $\sigma_i$ is the ionisation cross-section of the species "$I$". The multiplier gain, the electron energy and the multiplier are kept constant throughout the experiments. The instrument constant $K$ was determined by measuring ion intensity at $m/z = 32$ over the phase field $Fe_2O_3(s) + Fe_3O_4(s)$ in the temperature range 1146–1249 K and comparing the same with the literature data [11]. The ionisation cross-section data of $O_2^+$ corresponding to 70 eV was taken from Mann's tables [12].

Phase mixtures of $\{Fe_2O_3(s) + Fe_3O_4(s)\}$, $\{Rh_2O_3(s) + Rh(s)\}$ and $\{CaRh_2O_4(s) + Rh(s) + CaO(s)\}$ were pelletised, sintered in argon atmosphere at 1000 K for a week and used for measurements. About 1 g of the sample was loaded in the Knudsen cell. The sample was then heated to the desired temperature of measurement. The ion optics parameters were optimised and kept fixed (i.e. electron energy 70 eV, filament current 8 A, gain $10^8$) for all sets of measurements. The ion intensities were monitored in Analog to Digital Convertor (ADC) units as a function of $m/z$ values. Initially the background ion intensity was evaluated and the peak corresponding to $O_2^+$ was found to be very low as can be seen from Fig. 3. The ion intensity at $m/z$ value corresponding to $O_2^+$ (32) was monitored for the phase field $\{Fe_2O_3(s) + Fe_3O_4(s)\}$, $\{Rh_2O_3(s) + Rh(s)\}$ and $\{CaRh_2O_4(s) + Rh(s) + CaO(s)\}$. The ion intensities measured for the experiments are reported after background correction. There is negligible fragmentation of $O_2^+$ to $O^+$ and the ion intensities observed for $m/z = 16$ is low.

### 2.3. The fluoride cell assembly

A stacked pellet assembly with the solid electrolyte and electrodes in the form of pellets and a common inert gas atmosphere over both electrodes was used for the construction of the fluoride cell as shown in the Fig. 2. The pellets were placed in the following stacking sequence: reference pellet, $CaF_2(s)$ pellet and sample pellet inside an alumina cup with a hole in the center through which the lead of the platinum disc sitting on it could be passed. This cup along with the pellets were spring loaded into a quartz tube at one end of which could be attached to hooks which were provided in the flange. The flange was also provided with 'O' ring seal

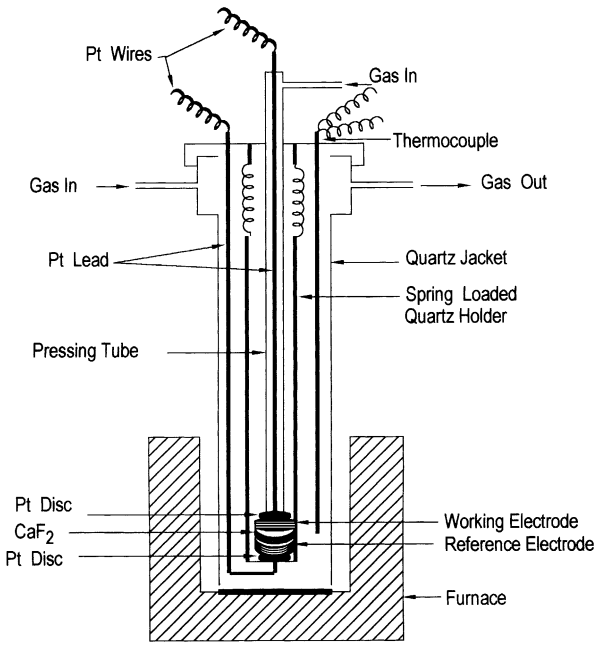


Fig. 2. Schematic diagram of the fluoride cell.

which could be tightened with the help of nuts and bolts. The entire set up was jacketed into another quartz tube to provide a leak proof atmosphere for the cell assembly.

The cell assembly was evacuated to $10^{-3}$ Pa at ambient temperature for several hours to remove all surface adsorbed moisture. The cell was then filled with dry nitrogen gas, and kept under flowing nitrogen. The nitrogen gas was purified to remove hydrogen and moisture by passing it sequentially over hot cupric oxide and a couple of towers of anhydrous magnesium perchlorate. The connections were made by using oxygen free high conducting copper tubing with brazed joints. The dried nitrogen gas contained about 100 ppm of oxygen and the flow rate was maintained at 1 $dm^3\,h^{-1}$ and provided the necessary gas atmosphere over the cell [10]. The cell was initially run using dry oxygen as the cover gas, flowing at the rate of 1 $dm^3\,h^{-1}$. However, in such a cell assembly it was found that over a period of time the emf of the cell started drifting. This was due to the formation of a fine black layer on the $CaF_2(s)$ pellet, causing the observed drift in emf. Hence, dry $N_2$ gas containing about 50–100 ppm. of oxygen was used as the gaseous atmosphere over the cell. Using this cover gas, drift in the emf was not observed even after a couple of hours. The outgoing cover gas was passed through a capillary tube immersed in silicone oil placed after the cell to protect the cell from back diffusion. The entire assembly was placed inside a vertical resistance furnace with the electrodes located in the even temperature zone of the furnace (±1 K) and a calibrated chromel-to-alumel thermocouple located in the vicinity of the stacked pellet assembly was used to monitor the cell temperature.

Optical grade single crystal of $CaF_2(s)$ (Harshaw/Filtrol, USA), dimension 9 mm diameter, 3 mm thickness was used

as the solid electrolyte. The reference electrode was made from an intimate mixture of CaO(s) and $CaF_2$(s) in the ratio 1:1 and compacted into a cylindrical pellet of diameter 7 mm and thickness 2–3 mm at a pressure of 100 MPa. The sample pellet was made similarly by compaction and pelletisation of a mixture of $\{CaF_2(s) + CaRh_2O_4(s) + Rh_2O_3(s)\}$ in the ratio of 1:1:1 into pellets of dimension 7 mm diameter and 3 mm thickness at a pressure of 100 MPa. emf of the cell was measured using a Keithley electrometer model-614, with high input impedance. The cell assembly was tested initially for the absence of asymmetric potential. The reproducibility of the emf data was verified by thermal cycling.

The following cell configuration was employed in the present study:

$$-Pt/O_2(g)\{CaO(s) + CaF_2(s)\}//CaF_2//\{CaRh_2O_4(s) + Rh_2O_3(s) + CaF_2(s)\}, O_2(g)/Pt + I$$

The cell is written in such a manner that the right hand electrode is positive. Measurements were carried out in the temperature range 879.7–1000 K. X-ray diffraction pattern of the pellet after electrochemical measurements did not reveal any interaction between the equilibrium oxide phases.

## 3. Results and discussion

### 3.1. Gibbs free energy of formation determined by using a quadrupole mass spectrometer coupled to a Knudsen cell

The background spectrum at 298.15 K at a pressure of $10^{-5}$ Pa can be seen in Fig. 3. The ion intensity of $O_2^+$ at $m/z = 32$ over the phase field $Fe_2O_3(s) + Fe_3O_4(s)$ was determined as a function of temperature in the range 1146–1249 K. There is no secondary ionisation of the oxygen species. A plot of ln(*IT*) versus 1/*T* should be a linear fit and the least squares regression analysis of the intensities obtained as a function of temperature can be given by the equation and given in Table 1.

$$\ln(IT) = \frac{-59\,889}{T\,(\mathrm{K})} + 60.23 \quad (2)$$

The relationship between pressure the machine constant and the ionisation cross-section can be given by

$$\ln(p) = \ln(IT) + \ln K + \ln \sigma_{(O_2)} \quad (3)$$

$$\ln(p) = \ln(IT) + K' \quad (4)$$

The $\ln(p(O_2))$ equation for $Fe_2O_3(s) + Fe_3O_4(s)$ obtained from the literature is

$$\ln p(O_2)\,(\mathrm{kPa}) = \frac{-59\,553.5}{T} + 38.861 \quad (5)$$

The constant $K'$ is obtained by a comparison of these two equations at an average experimental temperature of $T_{av} =$ 1197 K. The ionisation cross-section for oxygen at 70 eV was taken from Mann's tables [12]. Substituting these values in Eq. (3) we get $K'$.

$$K' = (\ln K + \ln \sigma_{(O_2)}) = -25.703 \quad (6)$$

This constant was used in the experiments involving the oxygen species. Using the above constant the partial pressure of oxygen over the phase field $Rh_2O_3(s) + Rh(s)$ was determined. The mass spectrum corresponding to $m/z = 32$ over the phase mixture was recorded as a function of temperature in the range 781.3–909.1 K. The least squares regression analysis of the intensities obtained as a function of temperature can be given by the linear equation given below:

$$\ln(IT) = \frac{-29\,124}{T\,(\mathrm{K})} + 45.037 \quad (7)$$

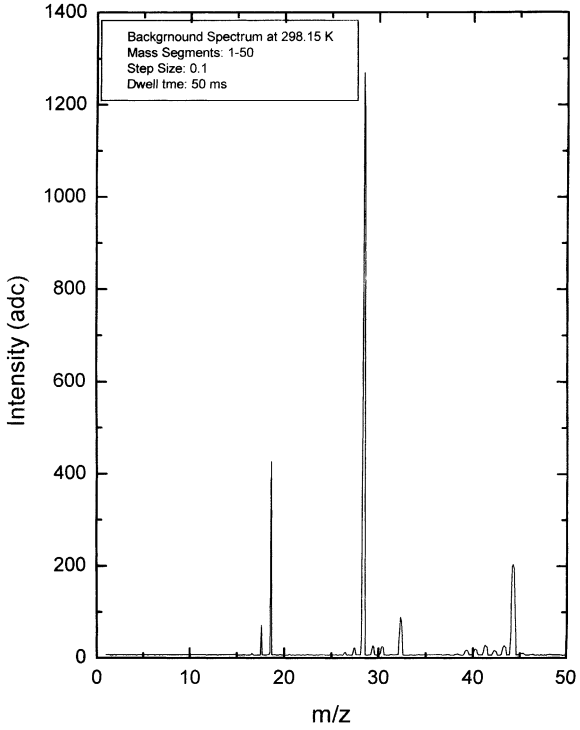


Fig. 3. Background spectrum taken at 298.15 K.

Table 1
Dependence of ln(*IT*) for the phase mixture $\{Fe_2O_3(s) + Fe_3O_4(s)\}$ on temperature

| *T* (K) | $(K/T) \times 10^4$ | ln(*IT*) |
|---|---|---|
| 1146 | 8.726 | 7.960 |
| 1161 | 8.613 | 8.516 |
| 1178 | 8.482 | 9.212 |
| 1190 | 8.403 | 10.324 |
| 1203 | 8.312 | 10.589 |
| 1204 | 8.305 | 10.389 |
| 1225 | 8.157 | 11.429 |
| 1230 | 8.130 | 11.497 |
| 1248 | 8.012 | 12.159 |
| 1249 | 8.006 | 12.230 |

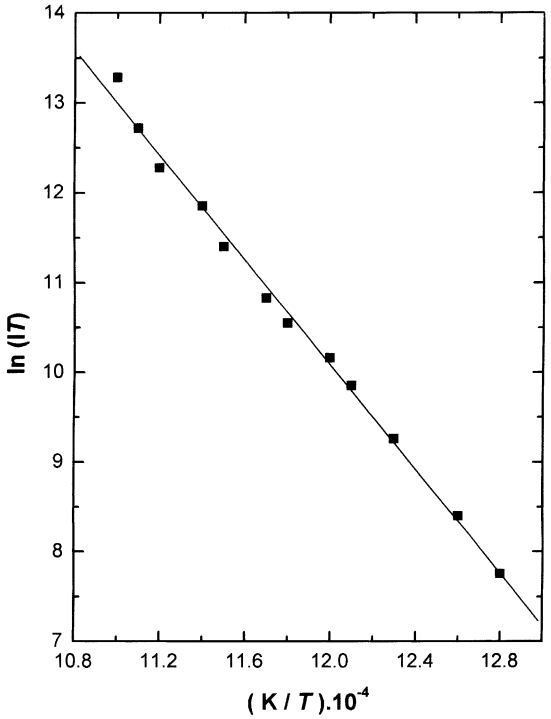


Fig. 4. Variation of ln(*IT*) as a function of reciprocal temperature for the phase mixture {$Rh_2O_3$(s) + Rh(s)}.

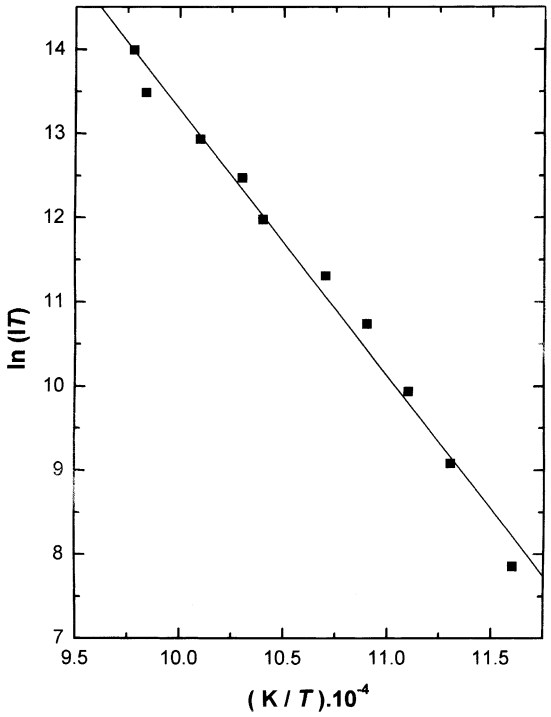


Fig. 5. Variation of ln(*IT*) as a function of reciprocal temperature for the phase mixture {CaO(s) + Rh(s) + $CaRh_2O_4$(s)}.

The plot of ln(*IT*) as a function of temperature is given in Fig. 4 and tabulated in Table 2. The partial pressure of oxygen has been calculated from Eq. (7) and the calibration constant. The expression obtained is given by

$$\ln p\,(\text{kPa}) = \frac{-29\,124}{T\,(\text{K})} + 23.948 \tag{8}$$

For the reaction: $2Rh(s) + 3/2O_2(g) = Rh_2O_3(s)$, the oxygen chemical potential can be given by

$$\mu(O_2)\,(\text{J mol}^{-1}) = RT \ln p(O_2) = -242\,140 + 160.7T\,(K) \tag{9}$$

Table 2
Variation of ln *p* (kPa) with temperature for the phase mixture {$Rh_2O_3$(s)+ Rh(s)}

| *T* (K) | (*K*/*T*) × $10^4$ | ln(*IT*) | ln *p* (kPa) |
|---|---|---|---|
| 781.3 | 12.8 | 7.756 | −13.328 |
| 793.7 | 12.6 | 8.400 | −12.684 |
| 813.0 | 12.3 | 9.262 | −11.822 |
| 826.4 | 12.1 | 9.852 | −11.232 |
| 833.3 | 12.0 | 10.163 | −10.921 |
| 847.5 | 11.8 | 10.548 | −10.536 |
| 854.7 | 11.7 | 10.831 | −10.253 |
| 869.6 | 11.5 | 11.400 | −9.684 |
| 877.2 | 11.4 | 11.852 | −9.232 |
| 892.9 | 11.2 | 12.279 | −8.805 |
| 900.9 | 11.1 | 12.717 | −8.367 |
| 909.1 | 11.0 | 13.286 | −7.798 |

$\Delta_f G^\circ$ ($Rh_2O_3$(s)) has been calculated and can be given by

$$\Delta_f G^\circ(Rh_2O_3(s))\,(\text{kJ mol}^{-1} \pm 2.0) = -363.2 + 0.241T\,(\text{K}) \tag{10}$$

Similarly the partial pressure of oxygen over the phase field $CaRh_2O_4(s) + Rh(s) + CaO(s)$ was determined in the temperature range 862.1–1022.7 K. The intensities of the peak corresponding to $m/z = 32.0$ as a function of temperature can be represented as

$$\ln(IT) = \frac{-31\,772.8}{T\,(\text{K})} + 45.065 \tag{11}$$

The plot of ln(*IT*) as a function of temperature is given in Fig. 5 and tabulated in Table 3. The partial pressure of

Table 3
Variation of ln *p* (kPa) vs. 1/*T* for the phase mixture {$CaRh_2O_4$(s) + Rh(s) + CaO(s)}

| *T* (K) | (*K*/*T*) × $10^4$ | ln(*IT*) | ln *p* (kPa) |
|---|---|---|---|
| 862.1 | 11.6 | 7.856 | −13.228 |
| 885.0 | 11.3 | 9.084 | −12.000 |
| 900.9 | 11.1 | 9.936 | −11.148 |
| 917.4 | 10.9 | 10.737 | −10.347 |
| 934.6 | 10.7 | 11.310 | −9.774 |
| 961.5 | 10.4 | 11.976 | −9.108 |
| 970.9 | 10.3 | 12.473 | −8.611 |
| 990.1 | 10.1 | 12.934 | −8.150 |
| 1016.0 | 9.84 | 13.485 | −7.599 |
| 1022.7 | 9.77 | 13.996 | −7.088 |

oxygen over the phase mixture has been calculated using Eq. (11) and the calibration constant and can be given by

$$\ln p\,(\mathrm{kPa}) = \frac{-31\,772.8}{T\,(\mathrm{K})} + 23.98 \quad (12)$$

For the reaction: $CaRh_2O_4(s) = CaO(s) + 2Rh(s) + 3/2O_2(g)$, the oxygen potential is

$$\mu(O_2)\,(\mathrm{kJ\,mol^{-1}}) = -264.16 + 0.161T\,(\mathrm{K}) \quad (13)$$

Using $\Delta_f G^\circ(CaO(s))$ from the literature [13] and Eq. (12), $\Delta_f G^\circ(CaRh_2O_4(s))$ has been calculated and can be given by

$$\Delta_f G^\circ(CaRh_2O_4(s))\,(\mathrm{kJ\,mol^{-1}} \pm 2.0) = -1030.5 + 0.3437T\,(\mathrm{K}) \quad (14)$$

### 3.2. Solid-state electrochemical measurements using fluoride cell

In the cell (I), $CaF_2(s)$ is the solid electrolyte. $CaF_2(s)$ is a fluorine ion conductor and the ionic transport number is greater than 0.99 at the temperature and fluorine partial pressure encountered in this study. The reversible emf of cell (I) is listed in Table 4, and the variation of emf as a function of temperature is shown in the Fig. 6. emf is a linear function of temperature, in the temperature range ($879.7 < T\,(\mathrm{K}) < 1000$). Within experimental uncertainty, the least square regression analysis gives

$$E\,(\mathrm{V})(\pm 7.63 \times 10^{-4}) = 0.3928 - 2.374 \times 10^{-4} T\,(\mathrm{K}) \quad (15)$$

The uncertainty quoted is the standard deviation in emf. The electrochemical reaction at the right hand side-working electrode can be written as

$$CaF_2(s) + Rh_2O_3(s) + \tfrac{1}{2}O_2(g) + 2e^- = CaRh_2O_4(s) + 2F^- \quad (\text{at the cathode}) \quad (16)$$

Table 4
Variation of emf of the cell: (−)Pt/$O_2$, {CaO(s) + $CaF_2$(s)}// $CaF_2$//{$CaF_2$(s) + $Rh_2O_3$(s) + $CaRh_2O_4$(s)}, $O_2$/Pt(+) as a function of temperature

| $T$ (K) | $E$ (V) |
|---|---|
| 879.7 | 0.1840 |
| 901.3 | 0.1789 |
| 909.0 | 0.1778 |
| 921.0 | 0.1741 |
| 930.0 | 0.1721 |
| 947.0 | 0.1664 |
| 971.0 | 0.1625 |
| 979.0 | 0.1609 |
| 986.0 | 0.1587 |
| 1000.0 | 0.1556 |

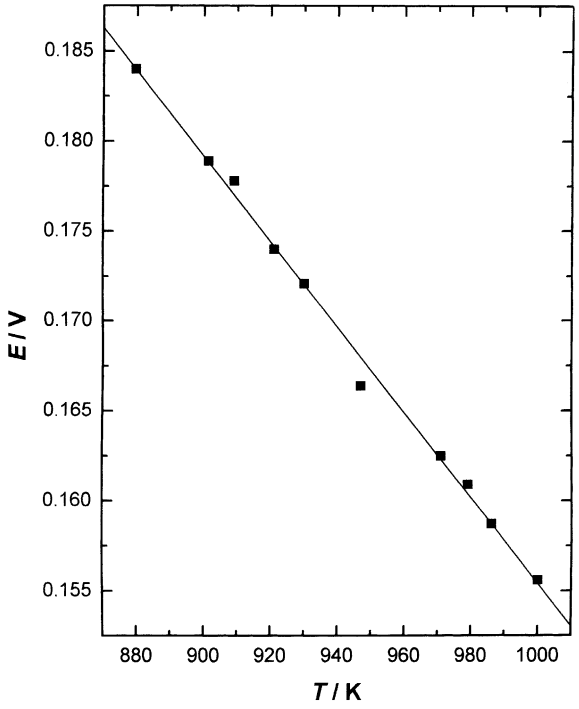


Fig. 6. Variation of emf of the cell: (−)Pt/$O_2$, {CaO(s) + $CaF_2$(s)}// $CaF_2$//{$CaF_2$(s) + $Rh_2O_3$(s) + $CaRh_2O_4$(s)}, $O_2$/Pt(+) as a function of temperature.

The electrochemical reaction at the reference electrode on the left-hand side of cell I can be written as

$$CaO(s) + 2F^- = CaF_2(s) + \tfrac{1}{2}O_2(g) + 2e^- \quad (\text{at the anode}) \quad (17)$$

The net cell reaction for the passage of two Faradays of electricity obtained by combining the two half cell reactions can be given by the following equation:

$$CaO(s) + Rh_2O_3(s) = CaRh_2O_4(s) \quad (18)$$

The standard Gibbs free energy change $\Delta_r G^\circ(T)$ for the above reaction, can be written as

$$\Delta_r G^\circ(T) = \Delta_f G^\circ(CaRh_2O_4)(s) - \Delta_f G^\circ(CaO(s)) - \Delta_f G^\circ(Rh_2O_3(s)) = -2FE \quad (19)$$

where $F$ is the Faraday constant $96\,486.4\,\mathrm{C\,mol^{-1}}$ and the condensed phases are at unit activity. The $\Delta_f G^\circ$ for Eq. (19) can be obtained by using $\Delta_f G^\circ(CaO(s))$ [13] and $\Delta_f G^\circ(Rh_2O_3(s))$ [13] and Eq. (15). $\Delta_f G^\circ(CaRh_2O_4(s))$ has been calculated and can be given by

$$\Delta_f G^\circ(CaRh_2O_4(s))\,(\mathrm{kJ\,mol^{-1}} \pm 2.0) = -1079 + 0.390T\,(\mathrm{K}) \quad (879.7 < T\,(\mathrm{K}) < 1000) \quad (20)$$

The slope and intercept of this least squares line corresponds, respectively, with the standard molar enthalpy

Table 5
Comparison of $\Delta_f G_m^\circ(T)$ of $Rh_2O_3$(s) from elements in their standard state, obtained by QMS coupled to Knudsen cell and oxide cell [9]

| Ref. | Method | $\Delta_f G_m^\circ(T)$ (kJ mol$^{-1}$) | | |
|---|---|---|---|---|
| | | $T = 800$ K | $T = 900$ K | $T = 1000$ K |
| [9] | Oxide cell | −170.8 | −142.6 | −114.4 |
| Present study | QMS coupled to a Knudsen cell | −170.4 | −146.3 | −122.2 |

Table 6
Comparison of $\Delta_f G_m^\circ(T)$ of $CaRh_2O_4$(s) from elements in their standard state, obtained by fluoride cell, QMS coupled to Knudsen cell and oxide cell [9]

| Ref. | Method | $\Delta_f G_m^\circ(T)$ (kJ mol$^{-1}$) | | |
|---|---|---|---|---|
| | | $T = 800$ K | $T = 900$ K | $T = 1000$ K |
| [9] | Oxide cell | −815.5 | −775.9 | −736.3 |
| Present study | Fluoride cell | −767.0 | −728.0 | −689.0 |
| Present study | QMS coupled to a Knudsen cell | −755.5 | −721.2 | −686.8 |

$\Delta_f H_m^\circ(T_{av})$ and entropy of formation $\Delta_f S_m^\circ(T_{av})$ of $CaRh_2O_4$(s) at the average experimental temperature (940.0 K). The Gibbs free energy of formation of rhodium oxide obtained in the present study, obtained by using QMS coupled to a Knudsen cell match with those obtained by oxide cell [9] as can be seen from Table 5. The Gibbs free energy of formation of calcium rhodite obtained in the present study, by fluoride cell match well with those obtained by using QMS coupled to a Knudsen cell. However, the Gibbs free energy values obtained by oxide cell [9] differ from values obtained by the present study by about 50 kJ mol$^{-1}$ as can be seen from Table 6.

## 4. Conclusion

A quadrupole mass spectrometer coupled to a Knudsen cell assembly has been used to measure the partial pressure of oxygen over the phase field $Rh_2O_3(s) + Rh(s)$ and $CaRh_2O_4(s) + Rh(s) + CaO(s)$. The Gibbs energy of formation of $Rh_2O_3$(s) from elements in their standard state in the temperature range 793.7–909.1 K can be given by $\{\Delta_f G^\circ(Rh_2O_3(s)) \pm 1.0\}$ (kJ mol$^{-1}$ $\pm$ 2.0) $= -363.2 + 0.241T$ (K). The Gibbs energy of formation of $CaRh_2O_4$(s) from elements in their standard state in the temperature range 862.1–1022.7 can be given by $\{\Delta_f G^\circ(CaRh_2O_4(s)) \pm 2.0\}$ (kJ mol$^{-1}$) $= -1030.5 + 0.3437T$ (K). A solid state electrochemical cell using $CaF_2$(s) as the solid electrolyte was used to measure the oxygen potential over the coexisting phase field $CaRh_2O_4(s) + Rh_2O_3(s) + CaF_2(s)$. The Gibbs energy of formation of $CaRh_2O_4$(s) from elements in their standard state was calculated by the least squares regression analysis of the data obtained in the present study and data for binary oxides from the literature and can be given by $\{\Delta_f G^\circ(CaRh_2O_4(s)) \pm 2.0\}$ (kJ mol$^{-1}$) $= -1079 + 0.390T$ (K) in the temperature range ($879.7 < T$ (K) $< 1000$).

## Acknowledgements

The authors are grateful to Dr. K.D. Singh Mudher for assisting with X-ray diffraction analysis.

## References

[1] H. Jehn, J. Less Comm. Met. 100 (1984) 321.
[2] A. Saric, S. Popovic, R. Trojko, S. Music, J. Alloys Comp. 320 (2001) 140.
[3] H. Kleykamp, Nucl. Technol. 80 (1988) 412.
[4] V.N. Skrobot, Russ. J. Inorg. Chem. 24 (1989) 1209.
[5] J. Nell, H.C.O. Neill, Geochim. Cosmochim. Acta 61 (1997) 4159.
[6] L. Wohler, N. Jochum, Z. Physik. Chem. N. F. 167 (1933) 169.
[7] K.T. Jacob, T. Uda, T.H. Okabe, Y. Waseda, High Temp. Mater. 19 (2000) 11.
[8] H. Kleykamp, Z. Physik. Chem. N. F. 67 (1969) 277.
[9] K.T. Jacob, Y. Waseda, J. Solid State Chem. 150 (2000) 213.
[10] V.A. Levitskii, J. Solid State Chem. 25 (1978) 9.
[11] G.V. Belov, B.G. Trusov, ASTD: Computer Aided Reference Book in Thermodynamical, Thermochemical and Thermophysical Properties of Species, Version 2.0 © 1983–1995, Moscow.
[12] J.B. Mann, J. Chem. Phys. 46 (1967) 1646.
[13] I. Barin, Thermochemical Data of Pure Substances, vol. I/II, third ed., VCH, New York, 1995.